Modeling, Filtering and Optimization for AFM Arrays

H. Hui*†
*School of Mechatronic Northwestern Polytechnical University,
127, Youyi Xilu, 710072 Xi'an Shaanxi, China
{hui.hui}@femto-st.fr

Y. Yakoubi
†FEMTO-ST, Time Frequency Department,
University of Franche-Comté,
26, Chemin de l'Epitaphe, 25030 Besançon Cedex, France

M. Lenczner
FEMTO-ST, Time Frequency Department,
University of Technology at Belfort and Montbéliard,
26, Chemin de l'Epitaphe, 25030 Besançon Cedex, France
{michel.lenczner}@utbm.fr

S. Cogan
FEMTO-ST,
Applied Mechanics Department, CNRS,
26, Chemin de l'Epitaphe, 25030 Besançon Cedex, France

A. Meister, M. Favre
CSEM,
Rue Jaquet-Droz 1 CH-2002 Neuchtel Switzerland

R. Couturier, S. Domas
University of Franche-Comte, LIFC, IUT Belfort-Montbliard,
Rue Engel Gros, 90000 Belfort, France

***Abstract*—In this paper, we present new tools and results developed for Arrays of Microsystems and especially for Atomic Force Microscope (AFM) array design. For modeling, we developed a two-scale model of cantilever arrays in elastodynamics. A robust optimization toolbox is interfaced to aid for design before the microfabrication process. A model based algorithm of static state estimation using measurement of mechanical displacements by interferometry is stated. Quantization of interferometry data processing is analyzed for FPGA implementation. A robust H_∞ filtering problem of the coupled cantilevers is solved for time-invariant system with random noise effects. Our solution allows semi-decentralized computing based on functional calculus that can be implemented by networks of distributed electronic circuits as shown in a previous paper.**

***Keywords*-Two-scale Model; Cantilevers Arrays; Parameter Optimization; Interferometry; Quantization Analysis; H_∞ Filtering;**

I. Introduction

Since its invention [1], Atomic Force Microscopes (AFM) have became very powerful tools for specimen imaging and nanomanipulation. But these devices suffer from relatively low speed of operation, and from low reliability of their measures. So, modeling and model-based optimization or filtering constitute a relevant issue to improve their performances. Now, a number of research laboratories are developing large arrays of AFMs, as this represented in Fig. 1, that achieve a same task in parallel, and improve operation speed. One of the design problems encountered in such systems comes from global effects namely from deformation of the common base mainly in static regime, and from cross-talk between cantilevers in dynamic regime. For model-based optimization or filtering, the full device must be represented by a single model. To prevent prohibitive computation time, in a previous work, we introduced a two-scale model yielding fast simulations. Now, we present our results related to parameter optimization, and to H_∞ filtering problem for real-time control of AFMs, both being based on our two-scale model.

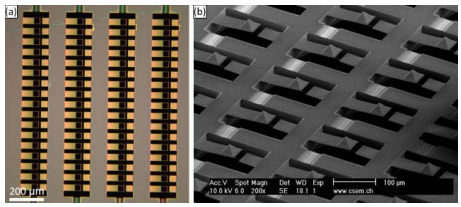

Fig. 1. (a) optical image of a 4 $\times$17 probe array with SiN cantilevers anchored on parallel-beam base. The dark square at the end of each cantilever corresponds to the pyramidalshaped tip. (b) SEM images of a probe arrays with SiN cantilevers anchored on a gridlike base.

Our simplified two-scale model has been introduced in [2], and its derivation is detailed in a submitted paper. It is rigorously justified thanks to an adaptation of the two-scale approximation method introduced in [3], and to further results in [4]. Its main advantage is that it requires little computing effort, and that it is reasonably precise for large arrays. A first investigation for real-time vibration control of a one-dimensional cantilever array has been carried out in the Linear Quadratic Regulation (LQR) framework. In view of real-time control applications, we have derived a *Semi-Decentralized Approximation* of the controller based on functional calculus, and formulated its realization through a *Periodic Network of Resistors*, see [5]. This approximation method has been carefully validated.

In this paper we focus on the filtering problem or state estimation. In the past decade, a number of linear filtering techniques have been developed for finite or infinite-dimensional

systems**.** In this paper, we formulate a model-based H_∞ filtering problem for an AFM array in a classical way but applied to an infinite dimensional system. The objective is to estimate the displacement in base though observing the displacement in cantilevers. We formulate the theoretical framework of functional calculus for computing the estimator in a semi-decentralized manner as in [5]. The numerical results are drawn from this formulation but obtained more directly using a modal decomposition instead of using the full framework of semi-decentralized approximation.

Regarding sensing, in some AFM arrays, the deflection of cantilever was measured by piezoresistive sensor integrated in the cantilever. In the paper [6], cantilever arrays equipped with piezoresistive sensors have been demonstrated in liquid environment. However, this approach suffers from the complexity of the microfabrication process of implementing the sensor in the cantilever. Additionally, the signal to noise ratio of piezoresistive arrays is limited due to the sensor noise. An interferometric readout method with imaging optics is provided in [7]. This approach does not suffer from optical cross-talk since the laser light reflected from one point on the cantilever is collected by only one pixel of the detector, and this independently of the direction the laser beam is reflected from the point. However, interferometry data processing requires heavy computation which represents a barrier to rapid operation. In order to FPGA implementation we study their quantization.

This paper is organized as follows. We state the simple two-scale model and its reformulation in Section II. Section III contains the robust parameter optimization. The measurement by interferometry is introduced in Section IV and is followed by a quantization analysis of its algorithm. Section V is dedicated to the static state estimation and an H_∞ filtering problem is formulated in Section VI. Numerical results for the H_∞ filtering problem are reported in Section VI-C.

II. A Two-scale Model for One-Dimensional AFM arrays

A. The Direct Model Formulation

We consider a one-dimensional cantilever array comprised of an elastic base, and a number of clamped elastic cantilevers with free end equipped with rigid tips. The whole array can be viewed as a periodic repetition of a same cell, in the two directions x_1 and x_2, see also Fig. 2 (a) for a one-dimensional view. The simplified model will be an approximation of the full model in the sense of small values of ε^*, the ratio of the cell size ε, to array size μ, i.e.

$$\varepsilon^* = \varepsilon/\mu. \tag{1}$$

To build it, we shall make use of the so-called two-scale approximation that we briefly introduce. Each point $x = (x_1, x_2, x_3)$ of the three-dimensional space is decomposed as

$$x = x^c + \epsilon y,$$

where x^c represents the coordinates of the center of the cell of x, $\epsilon = \begin{pmatrix} \varepsilon^* & 0 & 0 \\ 0 & \varepsilon^* & 0 \\ 0 & 0 & 1 \end{pmatrix}$, and $y = \epsilon^{-1}(x - x^c)$ is the dilated relative location of x with respect to x^c. Points with coordinates $y = (y_1, y_2, y_3)$ varying over the the unique so-called reference cell, that is obtained through a translation and the dilatation ϵ^{-1} of any current cell, see Fig. 2 (b) for a one-dimensional view of the reference cell. Assuming that the number of cantilevers is sufficiently large, a homogenized model was derived using a two-scale approximation method. This principle is exploited in the detailed paper [4] devoted to static regime. The corresponding model extended to dynamic regime is introduced in the letter [2]. Both papers were written in view of AFM application.

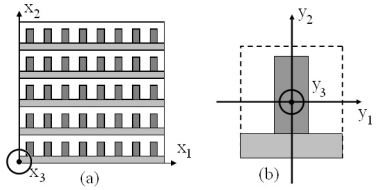

Fig. 2. A one-dimensional view of (a) an Array and (b) a reference cell

Our models are formulated from the Euler-Bernoulli beam model of the whole structure, and we will always assume that the ratio of cantilever thickness h_C to base thickness h_B is small, namely $\frac{h_C}{h_B} \approx \varepsilon^{*4/3}$. The simplified model is an approximation of the full model in the sense of small ε^*, the ratio of the cell size ε to array size μ; i.e. $\varepsilon^* = \varepsilon/\mu$. The two-scale approximation of deflection component of the vector of mechanical displacement fields is denoted by $u(t, x_1, y)$ where t represents the time variable. From the asymptotic analysis yielding the two-scale model, it appears that u is independent of y_3 everywhere. Moreover, we consider cantilevers made of an isotropic material and neglect variations of $y_1 \mapsto u(t, x_1, y)$. So their motions are governed by a classical Euler-Bernoulli beam equation in the microscopic space variable y_2,

$$m^C \partial^2_{tt} u + r^C \partial^4_{y_2 \dots y_2} u = F^C, \tag{2}$$

with m^C their linear mass density, r^C their linear stiffness coefficient, and F^C their load per unit length. This model holds for all x_1, and therefore represents motions of an infinite number of cantilevers parameterized by x_1. For y varying along the base, $y \mapsto u(t, x_1, y)$ is constant and therefore the displacement $u(t, x_1)$ is governed by an equation posed on a line $\Gamma = \{(x_1, y_2) | x \in (0, L_B) \text{ and } y_2 = 0\}$ where L_B is the base length in the macroscale x_1-direction,

$$\rho^B \partial^2_{tt} u + R^B \partial^4_{x_1 \cdots x_1} u + \ell_C r^C (\partial^3_{y_2 y_2 y_2} u)_{|junction} = f^B.$$

Here ρ^B, R^B, f^B and ℓ_C are respectively its effective length mass, its homogenized stiffness tensor, its effective load per unit surface, and the cantilever width in the reference cell. The base is assumed to be clamped, so the boundary conditions are

$u = \partial_{x_1} u = 0$ at both ends. The term $r^C(\partial^3_{y_2y_2y_2} u)_{|junction}$ is a distributed load originating from shear forces exerted by cantilevers at the base at base-cantilever junctions. Base-cantilever junction condition states as $u_{|cantilever} = u_{|base}$ and $\partial_{y_2} u_{|cantilever} = 0$. Other cantilever ends are equipped with a rigid part (the tip of Atomic Force Microscopes), thus

$$J^R \partial^2_{tt} \begin{pmatrix} u \\ \partial_{y_2} u \end{pmatrix} + r^C \begin{pmatrix} -\partial^3_{y_2y_2y_2} u \\ \partial^2_{y_2y_2} u \end{pmatrix} = \begin{pmatrix} f_3 \\ f_3(y_2^{tip} - L_C) \end{pmatrix} \tag{3}$$

at junctions between elastic parts and rigid parts. Here, J^R is a matrix of moments and f_3 is a point load at the tip apex located at $y_2 = y_2^{tip}$ in the microscale domain.

B. Base/Cantilever Displacement Decomposition

We introduce the extension $y \mapsto \overline{u}(.,y)$ of the restriction $y \mapsto u_{|base}(.,y)$ the displacement in base (which is in fact independent of y) to the values taken by y in cantilevers. We write the two-scale model in the static regime based on the decomposition of the two-scale displacements u as a sum of $\overline{u}$ the displacements in the base and $\widetilde{u}$ the displacements in the cantilevers: $u = \overline{u} + \widetilde{u}$. In the base, it is obvious that $\widetilde{u} = 0$ and $\nabla_y \overline{u} = 0$ since $\overline{u}$ is independent of y. We formulate the equations satisfied by the couple $(\overline{u}, \widetilde{u})$,

$$\begin{cases} \rho^B \partial^2_{tt} \overline{u} + R^B \partial^4_{x_1 \cdots x_1} \overline{u} \\ + \ell_C r^C (\partial^3_{y_2y_2y_2} \widetilde{u})_{|junction} = f^B, \text{ in base} \\ m^C \partial^2_{tt} \widetilde{u} + m^C \partial^2_{tt} \overline{u} \\ + r^C \partial^4_{y_2 \ldots y_2} \widetilde{u} = F^C, \text{ in cantilever} \end{cases} \tag{4}$$

In practice we will work on a model reduced at the microscopic scale through modal decompositions on cantilever modes $\{\phi_k(y_2)\}_{k=1..N}$ in $L^2(0, L_C)$, where the parameter L_C represent the cantilever length in the microscale domain, $\widetilde{u}(t, x_1, y_2) \approx \sum_{k=1}^{N} \widetilde{u}_k(t, x_1)\phi_k(y_2)$ and $F^C(t, x_1, y_2) \approx \sum_{k=1}^{N} f_k^C(t, x_1)\phi_k(y_2)$. In this approximation, equations (4) yields,

$$\begin{cases} \rho^B \partial^2_{tt} \overline{u} + R^B \partial^4_{x_1 \cdots x_1} \overline{u} \\ + \ell_C r^C (\partial^3_{y_2y_2y_2} \widetilde{u})_{|junction} = f^B \text{ in base,} \\ m^C \partial^2_{tt} \widetilde{u}_k + m^C \partial^2_{tt} \bar{u} \phi_k \\ + r^C \frac{\lambda_k^C}{(L_C)^4} \widetilde{u}_k = f_k^C \text{ for each } k, \end{cases} \tag{5}$$

where $\bar{\phi}_k = \int_0^{L_C} \phi_k \, dy_2$ and $\phi_k(y_2) = \varphi_k(y_2/L_C)$. The eigenelements $(\lambda_k, \varphi_k)_{k \in \mathbb{N}}$ are solutions to the eigenvalue problem, posed in $(0, 1)$,

$$\begin{cases} \varphi_k'''' = \lambda_k^C \varphi_k \quad \text{in } (0,1) \\ \varphi_k(0) = \varphi_k'(0) = 0, \quad \text{at } 0 \\ \begin{pmatrix} -\varphi_k''' \\ \varphi_k'' \end{pmatrix} = \lambda_k Q \begin{pmatrix} \varphi_k \\ \varphi_k' \end{pmatrix} \quad \text{at } 1. \end{cases}$$

where $Q = N \begin{pmatrix} J_0 & J_1 \\ J_1 & J_2 \end{pmatrix} N$ with $N = \begin{pmatrix} 1 & 0 \\ 0 & 1/L_C \end{pmatrix}$ and $J_i = \int_{Y_R} (y_2 - L_C)^i \, dy$, $i = \{0, 1, 2\}$.

III. The Robust Parameter Optimization Toolbox

The parameters of the array, such as the length, spring constant and deflection angle of the cantilevers, footprint of the array, must satisfy requirements for good operation. Thanks to a recent development design decision making tools, we can perform sensitivity, multi-objective optimization, as well as uncertainty quantification and robustness analysis. The objective of these tools is to support the analyst in specifying an AFM array design which meets the performance requirements in the presence of uncertainty due to both manufacturing tolerances and lack of knowledge in the modeling process. In this paper, we illustrate a design optimization problem for a one-dimensional array of cantilevers, see Fig. 3. The inputs

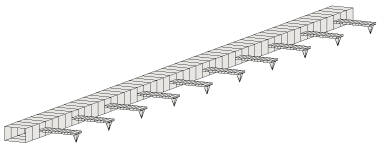

Fig. 3. One-dimensional Cantilever arrays with tips

of the design problem are the length, width and thickness of the cantilevers and the width and thickness of the base. The outputs of the problem are the static displacement at base F_Base and at tip apexes F_Tapex, the gap between two cantilevers F_Gap and the ratio of the void part to the area of each cell $F\_Gapcell$. The objective of this problem is to design an array to make F_Gap and $F\_Gapcell$ as large as possible, and F_Base as small as possible. In consideration of the requirement of micro-fabrication, three nonlinear constraints C_Angle, C_Gap and $C\_Gapcell$ are chosen as: the static cantilever deflection angle should be smaller than three degrees, and F_Gap and $F\_Gapcell$ must be more than half of the cantilever width and 0.4 respectively. In Fig. 4, we present the evolution of the objectives and constraints based on the mono-objective analysis. It is shown that the objectives are minimized and all the constraints are negative. Fig. 5 shows the

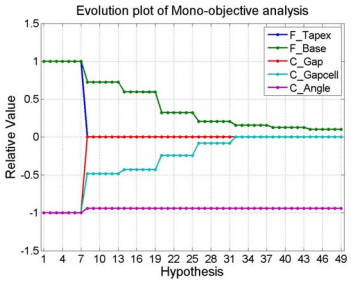

Fig. 4. Evolution plot of the objectives and constraints

convergence of a Pareto front for the two objective functions F_Gap and $F\_Gapcell$ based on Monte-Carlo sampling in multi-objective optimization problem. From this figure, the engineer can decide which compromise of the two objectives is most acceptable.

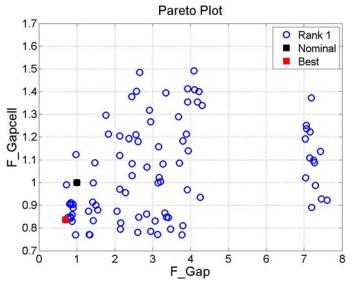

Fig. 5. Multi-objective analysis with Monte-Carlo sampling

IV. Measurement by Interferometry

The setup of the measurement scheme is an interferometric system. It is sensitive to the optical path difference induced by the vertical displacements of cantilevers, see Fig. 6. In

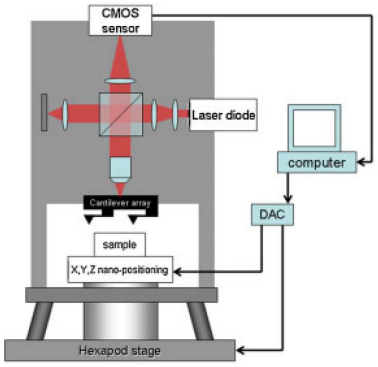

Fig. 6. Experimental set-up (sketch and picture) of the instrument for parallel AFM using two-dimensional probe arrays.

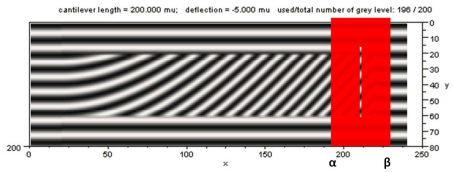

Fig. 7. Fringes and profile intensity of the cantilever

each cantilever, we neglect the variations of displacements u with respect to x_1. We write the intensity of a fringe pattern written in the two-scale frame,

$$I(t, x_1, y_2) = A\cos\left(2\pi f x_1 + \theta(t, y_2)\right) \text{ with } \theta = \frac{2\pi}{\bar{\lambda}}(b - u).$$

It is measured in a band perpendicular to the cantilever axis and parameterized by $y_2 \in (\alpha, \beta)$ as represented in Fig. 7. The parameters f and θ are two unknowns representing the spatial carrier frequency and the phase modulation of fringes, A is the modulation amplitude, $\bar{\lambda}$ is the wave-length and b is related to the constant path difference between the two interfering waves. An algorithm was developed to determine both the spatial frequency f and the phase modulation θ which yields an approximation of the average displacement along the measurement zone

$$Y = \frac{1}{|\beta - \alpha|}\int_{\alpha}^{\beta} u(x_1, y_2)\ dy_2 \tag{6}$$

which is used hereafter in the static state estimation and filtering problems.

The algorithm, determining the spatial frequency f (or period $T = \frac{1}{f}$) and the phase θ, is intended to be implemented on a quite small FPGA, where computations will be achieved out using integers only. Initially, the algorithm was written using high level functions. All steps have been rewritten and simplified in order to minimize costly operations as divisions, and to use integer numbers instead of floating point numbers (quantization). This was achieved by multiplying each number by a same power of 2 (referred as the *scaling factor*) and then by truncation. We compare the two algorithms. Figure 8 shows experiment results helping in determining the scaling factor insuring the best compromise between not being too small that decreases the precision and not too large which yields implementation problems in particular for multiplications. They were carried out for three pairs of periods and phases (rad) $(\frac{1}{f}, \theta) \in \{(4.5, 1),\ (3.5, 0.1),\ (3, 0.2)\}$. The curves represents the percentage errors for phase with respect to the power of the scaling factor. The error is constant for scaling factors above 2^6. Figure 9 represents the percentage errors between the phases provided by the algorithm using floating point numbers and the one using integer numbers based on a 2^8 scaling factor. Experiments are reported for three periods $\frac{1}{f} \in \{6, 4.5, 3\}$ and for phases varying between 0 and $\frac{\pi}{2}$.

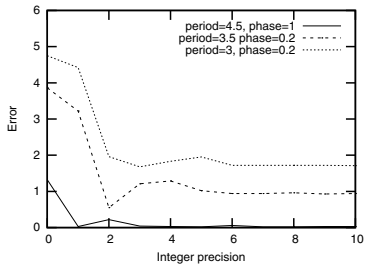

Fig. 8. Error percentage of phase calculation with respect to the scaling factor

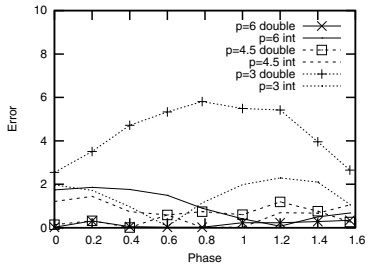

Fig. 9. Error of quantization on phases varying in $(0, \pi/2)$ for 3 values of the period (p)

V. Static State Estimation

We provide the mean to estimate base displacements from interferometric measurements in cantilevers using our two-scale model in the static operating regime. The latter is derived by eliminating the time terms from the elastodynamics model, presented in Section II. We assume that there is no body load i.e. $F^C = 0$ which yields the analytical solution

$$\widetilde{u}(x_1, y_2) = \frac{y_2^2}{6r^C}\left(3y_2^{tip} - y_2\right) f_3$$

where y_2^{tip} is the tip position. We require two measures along two parallel lines $y_2 = y_2^{0,1}$ and $y_2 = y_2^{0,2}$ corresponding to two phases θ_1 and θ_2 to build their difference $\delta\theta = \theta_2 - \theta_1$. We observe that $u(x_1, y_2^{0,2}) - u(x_1, y_2^{0,1}) = \widetilde{u}(x_1, y_2^{0,2}) - \widetilde{u}(x_1, y_2^{0,1}) = -\frac{\bar{\lambda}\delta\theta}{2\pi}$ which yields an expression of the tip force $f_3 = -\frac{\bar{\lambda}\delta\theta}{2\pi(K(y_2^{0,2}) - K(y_2^{0,1}))}$. From this force we can determine the base displacement from the elasto-static equation.

VI. Robust Filtering

A. Filtering Problem Statement

For the filtering problem in AFM array application we take into account unknown noise associated to interferometry measurements as well as other noise sources as air or liquid environment, thermal effect, electromagnetic noise. To deal with these uncertainties, we uses an H_∞ theory which is based on the worst case approach. We set $U^N = (\overline{u}, (\widetilde{u}_k)_{k=1,..,N}, \partial_t\overline{u}, (\partial_t\widetilde{u}_k)_{k=1,..,N})^T$ the state variable, $\mathcal{A}^N = \begin{pmatrix} 0 & 0 & I & 0 \\ 0 & 0 & 0 & I \\ -A_{x_1} & -A^N_{x_1y} & 0 & 0 \\ A_{x_1}\bar{\phi}_k & -A^N_y & 0 & 0 \end{pmatrix}$ the state operator, with $A_{x_1} = \frac{R^B}{\rho^B}\partial^4_{x_1\cdots x_1}$, $A^N_{x_1y} = \frac{\ell_C r^C}{\rho^B}(\partial^3_{y_2y_2y_2}\phi_k(0))_{k=1,..,N}$ and $A^N_y = \left(-\frac{\ell_C r^C}{\rho^B}\partial^3_{y_2y_2y_2}\phi_k(0)\bar{\phi}_k + \frac{r^C}{m^C(L_C)^4}\lambda^C_k\right)_{k=1,..,N}$, $\mathcal{B}^N = \begin{pmatrix} 0 & 0 & I & 0 \\ 0 & 0 & 0 & I \end{pmatrix}^T$ the perturbation operator. The perturbations in the state system being denoted by $w_1^N \in \mathcal{W}_1 = L^2(\Gamma) \times L^2(\Gamma)^N$, the state equation is

$$\partial_t U^N = \mathcal{A}^{\mathcal{N}} U^N + \mathcal{B}^N w_1^N \text{ for } t \in \mathbb{R}^+ \text{ and } U^N(0) = U_0^N.$$

Here $\mathcal{A}^N$ is the infinitesimal generator of a continuous semigroup on the separable Hilbert space $\mathcal{H} = H_0^2(\Gamma) \times L^2(\Gamma)^N \times L^2(\Gamma) \times L^2(\Gamma)^N$ with dense domain $D(\mathcal{A}^N) = H^4(\Gamma) \cap H_0^2(\Gamma) \times L^2(\Gamma)^N \times H_0^2(\Gamma) \times L^2(\Gamma)^N$. The perturbations operator $\mathcal{B}^N \in \mathcal{L}(\mathcal{W}_1, \mathcal{H})$.

The observation comes from interferometry measurement as in (6) but take into account an additional unknown noise w_2. Then, using the modal decomposition with respect to y_2, the noise disturbed measurement turns to be given by

$$Y^N = \mathcal{C}^N U^N + \mathcal{D}^N w_2^N \in \mathcal{Y} = L^2(\Gamma)$$

the space of measurements, with the observation operator $\mathcal{C}^N = \left(I \quad \frac{1}{\beta-\alpha}\left(\int_\alpha^\beta \phi_k \, dy_2\right)_{k=1,..N} \quad 0 \quad 0\right) \in \mathcal{L}(\mathcal{H}, \mathcal{Y})$, $w_2^N \in \mathcal{W}_2$, and the weight operator for the measurement noise $\mathcal{D}^N = I \in \mathcal{L}(\mathcal{W}_2, \mathcal{Y})$. We assume that $(\mathcal{A}^N, \mathcal{B}^N)$ is stabilizable and that $(\mathcal{C}^N, \mathcal{A}^N)$ is detectable. The output operator is $L : \mathcal{H} \longrightarrow \mathcal{Z}$, and the partial state to be estimated is

$$Z^N = LU^N.$$

Here, we estimate the displacement at base, so $L = \begin{pmatrix} I & 0 & 0 & 0 \end{pmatrix}$ and $\mathcal{Z} = H_0^2(\Gamma)$. We define the estimation $\widehat{Z}^N$ of Z^N and the worst-case performance measures as

$$J = \sup_{(U_0^N, \mathcal{W}_1 \times \mathcal{W}_2)} \frac{||Z^N - \widehat{Z}^N||^2_{\mathcal{Z}}}{||w_1^N||^2_{\mathcal{W}_1} + ||w_2^N||^2_{\mathcal{W}_2}}.$$

The filtering problem is stated as: Given $\gamma > 0$, find a filter $Y^N \longrightarrow Z^N$, such that $J < \gamma^2$. This problem has a solution if and only there exists a unique self-adjoint non-negative solution P to the operational Riccati equation,

$$\begin{array}{l}(\mathcal{A}^N P + P\mathcal{A}^{N*} - P\mathcal{C}^{N*}\mathcal{C}^N P \\ +\frac{1}{\gamma^2} PL^*LP + \mathcal{B}^N\mathcal{B}^{N*})z = 0,\end{array} \tag{7}$$

for all $z \in D(\mathcal{A}^{N*})$. The adjoint $\mathcal{A}^{N*}$ of the unbounded operator $\mathcal{A}^{N*}$ is defined from $D(\mathcal{A}^{N*}) \subset \mathcal{H}$ to $\mathcal{H}$ by the equality $(\mathcal{A}^{N*}z, z')_{\mathcal{H}} = (z, \mathcal{A}^N z')_{\mathcal{H}}$ for all $z \in D(\mathcal{A}^{N*})$ and $z' \in D(\mathcal{A}^N)$. The adjoint $\mathcal{B}^{N*} \in \mathcal{L}(\mathcal{H}, \mathcal{W}_1)$ of the bounded operator $\mathcal{B}^N$ is defined by $(\mathcal{B}^{N*}z, w)_{\mathcal{W}_1} = (z, \mathcal{B}^N w)_{\mathcal{H}}$, the adjoint $\mathcal{C}^{N*} \in \mathcal{L}(\mathcal{Y}, \mathcal{H})$ being defined similarly. The filter $Y^N \mapsto \widehat{Z}^N$ is given as follows

$$\begin{array}{rcl}\partial_t\widehat{U}^N & = & \mathcal{A}^N\widehat{U}^N + K(Y^N - \mathcal{C}^N\widehat{U}^N),\ \widehat{U}^N(0) = 0, \\ \widehat{Z}^N & = & L\widehat{U}^N \quad \text{for } t \in \mathbb{R}^+,\end{array} \tag{8}$$

where the filter gain is $K = P\mathcal{C}^{N*}$.

B. Functional Calculus Based Approximation

This subsection is devoted to apply the approximation method introduced in [8] and [9]. We denote by Λ, the mapping: $\Lambda : f \longrightarrow v$, where v is the unique solution of $\partial^4_{x_1\cdots x_1} v = f$ in Γ with the boundary conditions $v = \partial_{x_1} v = 0$ for $x_1 = \{0, L_B\}$. The spectrum $\sigma(\Lambda)$ is discrete and made up of positive real eigenvalues λ_k. They are solutions to the eigenvalue problem $\Lambda\phi_k = \lambda_k\phi_k$ with $||\phi_k||_{L^2(\Gamma)} = 1$. In the sequel, $I_\sigma = (\sigma_{\min}, \sigma_{\max})$ refers to an open interval that includes the complete spectrum. For a given real valued function g, continuous on I_σ, $g(\Lambda)$ is the linear self-adjoint operator on the space $\mathcal{X} = L^2(\Gamma)$ defined by $g(\Lambda)z = \sum_{k=1}^{\infty} g(\lambda_k) z_k \phi_k$, where $z_k = \int_\Gamma z\phi_k \, dx$.

We introduce the factorization of the filter gain K under the form of a product of a matrix of functions of Λ. To do so, we introduce the change of variable operators $\Phi_H = \begin{pmatrix} \Lambda^{\frac{1}{2}} & 0 & 0 & 0 \\ 0 & I & 0 & 0 \\ 0 & 0 & I & 0 \\ 0 & 0 & 0 & I \end{pmatrix} \in \mathcal{L}\left(\mathcal{X}^{2N+2}, \mathcal{H}\right)$, $\Phi_W = I \in \mathcal{L}\left(\mathcal{X}^{N+1}, \mathcal{W}_1\right)$, $\Phi_Z = \Lambda^{\frac{1}{2}} \in \mathcal{L}(\mathcal{X}, \mathcal{Z})$, and $\Phi_Y = I \in \mathcal{L}(\mathcal{X}, \mathcal{Y})$, from which we introduce the matrices of functions of Λ, $a(\Lambda) = \Phi_H^{-1}\mathcal{A}^N\Phi_H$, $b(\Lambda) = \Phi_H^{-1}\mathcal{B}^N\Phi_W$, $c(\Lambda) = \Phi_Y^{-1}\mathcal{C}^N\Phi_H$ and $\ell(\Lambda) = \Phi_Z^{-1}L\Phi_H$, simple

to implement on a semi-decentralized architecture. A straightforward calculation yield $a(\lambda) = \begin{pmatrix} 0 & 0 & \lambda^{-1/2} & 0 \\ 0 & 0 & 0 & I \\ -a_{x_1} & -a^N_{x_1 y} & 0 & 0 \\ a_{x_1}\bar{\phi}_k & -a^N_y & 0 & 0 \end{pmatrix}$, $b(\lambda) = \begin{pmatrix} 0 & 0 \\ 0 & 0 \\ I & 0 \\ 0 & I \end{pmatrix}$, $c(\lambda) = \begin{pmatrix} \lambda^{1/2} & \frac{1}{\beta-\alpha}\left(\int_\alpha^\beta \phi_k \, dy_2\right)_{k=1..N} & 0 & 0 \end{pmatrix}$ and $\ell(\lambda) = \begin{pmatrix} I & 0 & 0 & 0 \end{pmatrix}$ where $a_{x_1} = \frac{R^B}{\rho^B}\lambda^{-1/2}$ $a^N_{x_1 y} = \frac{\ell_C r^C}{\rho^B}(\partial^3_{y_2 y_2 y_2}\phi_k(0))_{k=1,..,N}$ and $a^N_y = (-\frac{\ell_C r^C}{\rho^B}\partial^3_{y_2 y_2 y_2}\phi_k(0)\bar{\phi}_k + \frac{r^C}{m^C(L_C)^4}\lambda^C_k)_{k=1,..,N}$,. Endowing $\mathcal{H}$, $\mathcal{W}_1$, $\mathcal{Y}$ and $\mathcal{Z}$ with the inner products $(z,z')_{\mathcal{H}} = \left(\Phi_H^{-1}z, \Phi_H^{-1}z'\right)_{\mathcal{X}^{2N+2}}$, $(w,w')_{\mathcal{W}_1} = \left(\Phi_W^{-1}w, \Phi_W^{-1}w'\right)_{\mathcal{X}^{N+1}}$, $(y,y')_{\mathcal{Y}} = \left(\Phi_Y^{-1}y, \Phi_Y^{-1}y'\right)_{\mathcal{X}}$ and $(\ell,\ell')_{\mathcal{Z}} = (\Phi_Z^{-1}\ell, \Phi_Z^{-1}\ell')_{\mathcal{X}}$, we find the subsequent factorization of the filter gain K in (8) which plays a central role in the approximation. The approximation of the functions of Λ is detailed in [5].

Proposition 1: The filter gain K admits the factorization $K = \Phi_H \; p \; c^T \; \Phi_Y$, where $p(\lambda)$ is the unique symmetric non-negative matrix solving the algebraic Riccati equation

$$ap + pa^T - p(c^T c - \frac{1}{\gamma^2}\ell^T\ell)p + bb^T = 0.$$

Remark 1: We indicate how the isomorphisms Φ_H, Φ_Y, Φ_W and Φ_Z have been chosen. The choice of Φ_H comes directly from the expression of the inner product $(z,z')_{\mathcal{H}} = \left(\Phi_H^{-1}z, \Phi_H^{-1}z'\right)_{\mathcal{X}^{2N+2}}$ and from $(z_1,z_1')_{H_0^2(\Gamma)} = \left((\Delta^2)^{\frac{1}{2}}z, (\Delta^2)^{\frac{1}{2}}z'\right)_{L^2(\Gamma)}$. The choice of Φ_Z is similar. For Φ_Y, we start from $\mathcal{C}^N = \Phi_Y c(\Lambda)\Phi_H^{-1}$ and from the relation $(y,y')_{\mathcal{Y}} = \left(\Phi_Y^{-1}y, \Phi_Y^{-1}y'\right)_{\mathcal{X}}$ which implies that $1 = (\Phi_Y)_{1,1}c_{1,1}(\Lambda)\Lambda^{-\frac{1}{2}}$. The expression of Φ_Y follows. Choosing Φ_W is straightforward.

C. An Illustrative Example

We present the numerical results of the H_∞ filtering problem for a silicon array comprised of 10 elastic cantilevers. The base dimensions are $L_B \times l_B \times h_B = 500\mu m \times 16.7\mu m \times 10\mu m$, and those of cantilevers are $L_C \times l_C \times h_C = 25\mu m \times 10\mu m \times 1.25\mu m$. The other model parameters are the bending coefficient $R^B = 1.09 \times 10^{-5} N/m$, $R^C = 2.13 \times 10^{-4} N/m$ and the masses per unit length $\rho^B = 0.0233 kg/m$, $\rho^C = 0.00291 kg/m$. We set the initial condition $U^N(0) = \begin{pmatrix} 10^{-6} & 10^{-6} & 10^{-6} & 0 & 0 & 0 \end{pmatrix}^T$ and $\gamma = 1.2$. The computation is based on a modal decomposition of Λ with 10 modes together with 2 cantilever modes. In this example, the displacement are measured in the interval $(\alpha,\beta) = (36,40)\mu m$. The simulation have been carried out in the time interval $[0, 1\mu s]$ with a time step $0.1ns$. The comparison between the displacement and the estimated displacement in base is presented in Fig. 10 (a) and the estimation error is described in in Fig. 10 (b).

VII. Conclusions

In this paper, we have studied the problem of state estimation in an array of AFMs based on a two-scale model.

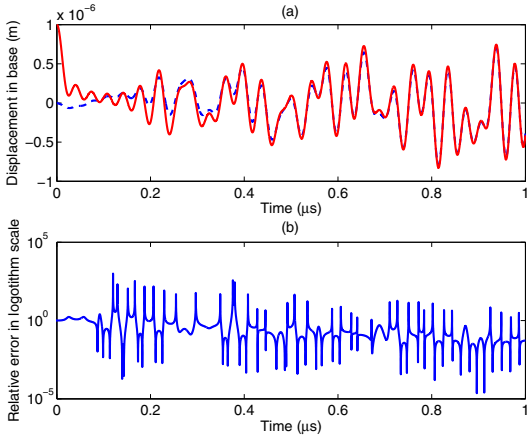

Fig. 10. (a) Comparison between true and estimated outputs (b) Absolute error between true and estimated outputs

The measurement of displacements is done by an interferometric readout method. Positive quantization results related to the algorithm of interferometry have been reported, they allow to consider its FPGA implementation in view of real-time measurements. The full solution of the state estimation in the base has been provided for static operating regime. For dynamic operating regime, we have stated the mathematical framework of functional calculus dedicated to semi-decentralized computation of the solution of a robust H_∞ filtering problem and shown encouraging preliminary results. Finally, an application of our toolbox of robust optimization made to illustrate the functionality it provides to a designer to achieve design objectives satisfying design requirements.

Acknowledgment

This work is partially supported by the European Territorial Cooperation Programme INTERREG IV A France-Switzerland 2007-2013.

References

[1] G. Binnig, C.F. Quate, and C. Gerber. Atomic force microscope. *Physical Review Letters*, 56(9):930 – 3, 1986.

[2] M. Lenczner. A multiscale model for atomic force microscope array mechanical behavior. *Applied Physics Letters*, 90:091908, 2007.

[3] M. Lenczner. Homogeneisation d'un circuit electrique. *C. R. Acad. Sci. Paris*, Serie II b, t. 324(9):537–542, 1997.

[4] M. Lenczner and R. C. Smith. A two-scale model for atomic force microscopes arrays in static operating regime. *Mathematical and Computer Modelling*, 46:776–805, 2007.

[5] H. Hui, Y. Yakoubi, M. Lenczner, and N. Ratier. Control of a cantilever array by periodic networks of resistances. Thermal, Mechanical and Multi-Physics Simulation, and Experiments in Microelectronics and Microsystems (EuroSimE), 2010 11th International Conference on 26-28 April 2010, Bordeaux France.

[6] Polesel-Maris J, Aeschimann L, Meister A, Ischer R, Bernard E, Akiyama T, Giazzon M, Niedermann P, Staufer U, Pugin R, de Rooij NF, Vettiger P, and Heinzelmann H. Piezoresistive cantilever array for life sciences applications. *J. Phys: Conf*, Ser 61:955–959, 2007.

[7] M. Favre, Jérôme Polesel-Maris, Thomas Overstolz, Philippe Niedermann, Stephan Dasena, Gabriel Gruener, Réal Ischera, Peter Vettiger, Martha Liley, Harry Heinzelmann, and André Meister. Parallel afm imaging and force spectroscopy using two-dimensional probe arrays for applications in cell biology. *Accepted in J. Mol. Recognit.*, 2011.

[8] M. Lenczner and Y. Yakoubi. Semi-decentralized approximation of optimal control for partial differential equations in bounded domains. *Comptes Rendus Mécanique*, 337:245–250, 2009.

[9] Y. Yakoubi. *Deux Méthodes d'Approximation pour un Contrôle Optimal Semi-Décentralisé pour des Systèmes Distribués*. PhD thesis, Université de Franche-Comté, 2010.